Molecular Crystals and Liquid Crystals Science and Technology. Section A. Molecular Crystals and Liquid Crystals

Publication details, including instructions for authors and subscription information:
http://www.tandfonline.com/loi/gmcl19

Measurement and Analysis of the Naphthalene — Octafluoronaphthalene Phase Diagram: Complex Formation in Solid and Liquid

F. Michaud [a], Ph. Negrier [a], D. Mikailitchenko [a], A. Marbeuf [a], Y. Haget [a], M. Cuevas-diarte [b] & H. A. J. Oonk [c]

[a] Centre de Physique Moléculaire Optique et Hertzienne, UMR 5798, CNRS-Université Bordeaux, I F-33405, Talence, Cedex, France

[b] Departament de Cristal. lografia, Universitat de Barcelona Marti i Franquès, E-080828, Barcelona, Spain

[c] Department of Interfaces and Thermodynamics, Faculty of Chemistry, Petrology Group, Faculty of Earth Sciences, Budapestlaan 4, 3584 CD, Utrecht, The Netherlands

Version of record first published: 24 Sep 2006

Mol. Cryst. Liq. Cryst., Vol. 326, pp. 409–424
Reprints available directly from the publisher
Photocopying permitted by license only

Measurement and Analysis of the Naphthalene – Octafluoronaphthalene Phase Diagram: Complex Formation in Solid and Liquid

F. MICHAUD[a], PH. NEGRIER[a], D. MIKAILITCHENKO[a], A. MARBEUF[a,*], Y. HAGET[a], M. CUEVAS-DIARTE[b] and H. A. J. OONK[c]

[a] *Centre de Physique Moléculaire Optique et Hertzienne, UMR 5798 CNRS-Université Bordeaux I F-33405 Talence Cedex, France;*
[b] *Departament de Cristal.lografia, Universitat de Barcelona Marti i Franquès E-080828 Barcelona, Spain;*
[c] *Department of Interfaces and Thermodynamics, Faculty of Chemistry, Petrology Group, Faculty of Earth Sciences, Budapestlaan 4 3584 CD Utrecht, The Netherlands*

(Received 24 March 1998; In final form 27 July 1998)

Naphthalene–octafluoronaphthalene room pressure solid–liquid phase diagram has been assessed by means of differential scanning calorimetry and powder X-ray diffraction analyses. Thermodynamic properties are analysed through the associated liquid model. The solid states consists of six crystalline phases with well defined composition: one for naphthalene, two for octafluoronaphthalene and three for an equimolecular intermolecular compound. This complex melts congruently at (406.3 ± 0.3) K, *i.e.*, about fifty degrees higher than its components and the resulting liquid is moderately associated. The solid–solid phase transitions of this complex are strongly energetic. The corresponding overall change of entropy stands for two third times the entropy of fusion. The consecutive increasing of crystalline symmetry and positional disorder is clearly visible on diffraction patterns.

Keywords: Octafluoronaphthalene; naphthalene; molecular complexes; associated liquid

* Corresponding author. Tel.: (33) 05 5684 6212, Fax: (33) 05 5684 6970.

I. INTRODUCTION

It is well known that polyfluorinated aromates tend to form intermolecular complexes with aromatic hydrocarbons [1–7]. A speaking example is the combination of benzene and hexafluorobenzene where the solid 1:1 complex appears as a precipitate when the two liquid components are mixed at room temperature [1].

Among the about thirty organic complexes actually identified, known complex compounds combine fluorobenzene with benzene and its derivatives. By means of a variety of thermodynamic methods, it has been shown that the complexes only partly dissociate on melting: in particular, the volume–[8–9], enthalpy–[10–13] and free energy changes [14–16] that accompany the mixing of the liquid components to a liquid mixture are strongly negative; moreover, molecular associations have been detected both in vapour [17] and liquid phase [18]. Investigations with different non-thermodynamic methods such as polarisability study of hydrocarbons [9, 19–22] and the evaluation of the permanent molecular quadrupolar moments [23–24] give an electrostatic origin for the complex stability. Molecular geometry and stacking effect would play an important role in the lattice stability: complex crystal structures consist of ordered mixed chains in a crystallographic direction [2, 8–9, 25–28].

In our research groups, the investigation of molecular complexes is part of a wider program on mixed molecular interactions–including also the interactions in mixed crystals of the substitutional type (see Ref. [29] for the case of naphthalene family). Up till now we have published on the formation of complexes in the following systems: binaries involving substituted benzene (chlorobenzene [13], toluene and paraxylene [30]) and hexafluorobenzene, 2-chloronaphthalene + octafluoronaphthalene [31].

The interest of studies in the naphthalene family, involving octafluoronaphthalene as one of the molecular partner is the complex lattice, lies mainly in the greater occurrence of strong *H*...*F* interactions than in benzene family. In particular, it would be interesting to investigate the naphthalene + octafluoronaphthalene system, where a 1:1 complex has been detected [7] without charge transfer [32–33], and to compare to its benzenic analogue in studying stability and polymorphism of the complex, liquid properties.

In this paper, an account is given of the results obtained for the complex forming system naphthalene + octafluoronaphthalene. The complete solid–liquid phase diagram was determined by means of differential scanning calorimetry and X-ray diffraction. In addition an assessment was made of the thermodynamic properties, using the phase diagram and the available thermochemical data.

The 1:1 complex in the system gives rise to three different crystalline forms.

II. EXPERIMENTAL

II.1. Materials

The naphthalene used was Eastman-Kodak Scintillation grade 13007, having a purity of over 99.9% by gas-chromatography in combination with mass spectrometry. Octafluoronaphthalene from Aldrich (24,806-1) had a purity, as indicated by the same method, of over 98%, the main contaminants being heptafluoronaphthalene and heptafluorochloronaphthalene. Octafluoronaphthalene was used without further purification.

The room temperature form of the complex was obtained as colourless needles by fast evaporation under a flow of nitrogen from a temperature-controlled solution in ether. Samples of about 1g of varying compositions were prepared by the same technique of evaporation as well as by quenching from the melt in sealed glass tubes.

II.2. Techniques

Transition temperatures and enthalpies were obtained by means of differential scanning calorimetry in heating experiments at a rate of $2\,K \cdot min^{-1}$ (see Ref. [34] for details). Two different instruments were used: Du Pont DSC 910/990 (sample mass 1.5 mg, indium as standard material) and Perkin-Elmer DSC7 (sample mass 4 mg, indium and naphthalene standards).

In addition to thermal analysis, phase diagram characteristics were also determined by means of X-ray isothermal powder diffraction. The instruments used were a Guinier-Simon camera (Enraf-Nonius) or a diffractometer in dispersive mode (Inel) : in both cases samples were enclosed in Lindemann tubes having a diameter of 0.5 mm and the monochromatized wavelength came from a Cu-anode ($\lambda = 1.54056$ Å).

III. RESULTS

III.1. The Pure Components

In the case of naphthalene there is just one crystalline form, the characteristics of which [35] are given in Table I. The thermochemical melting data of the substance are in Table II.

TABLE I Cell parameters, cell volume, number of formula units per cell and compacity ratio for crystalline phases in the naphthalene–octafluoronaphthalene system (all phases belong to the $P2_1/a$ space group)

Phase	*T* (*K*)	*a* (Å)	*b* (Å)	*c* (Å)	*β* (°)	*V* (Å^3)	*Z*	*k*	*Ref.*
A	293	8.262(3)	5.984(3)	8.117(5)	116.02(3)	360.6(9)	2	0.75	[35]
C_{III}	293	12.684(2)	8.497(2)	7.450(1)	99.39(2)	792.1(4)	2	0.74	this work
B_{II}	260	11.287(11)	4.674(36)	17.033(27)	107.34(57)	857.8(10)	4	0.73	[39]
B_I	293	11.948(2)	5.000(1)	7.603(1)	96.80(2)	451.0(3)	2	0.69	this work

TABLE II Phase transition temperatures, enthalpies and entropies (per mole of formula units) for the pure components and the complex in the naphthalene–octafluoronaphthalene system

Compound	*Transition*	*T* (*K*)	ΔH ($J \cdot mol^{-1}$)	ΔS ($J \cdot mol^{-1} \cdot K^{-1}$)
$C_{10}H_8$	$A \rightarrow L$	352.8 ± 0.4	18970 ± 250	53.2 ± 0.7
	$C_{III} \rightarrow C_{II}$	382.3 ± 0.4	11700 ± 500	30.6 ± 1.4
$C_{10}H_8 : C_{10}F_8$	$C_{II} \rightarrow C_I$	386.9 ± 0.3	5960 ± 200	15.4 ± 0.6
	$C_I \rightarrow L$	406.3 ± 0.3	26700 ± 1000	65.8 ± 2.6
$C_{10}F_8$	$B_{II} \rightarrow B_I$	283.6 ± 1.3	2120 ± 100	7.5 ± 0.4
	$B_I \rightarrow L$	358.8 ± 0.4	17550 ± 330	48.9 ± 1.0

Octafluoronaphthalene, on the other hand, is giving rise to two different solid forms [36–42], the low-temperature form B_{II} and the high-temperature form B_I: a typical pattern of the high-temperature form is shown in Figure 1. Crystallographic data are in Table I and thermochemical data in Table II. It can be observed that B_I is less compact than B_{II}, the latter having about the same compacity as crystalline naphthalene.

The transition on cooling from B_I to B_{II} is rather sluggish: it is not complete when the material is held of 20 min at 35 K below the transition temperature. Reproducible results free from thermal anomalies could be obtained after keeping the samples during 20 min at 173 K.

III.2. The 1:1 Complex

In the temperature range studied (150 K to 420 K), the 1:1 complex (*C*) shows three different forms, hereafter denoted C_{III}, C_{II} and C_I in order of increasing temperature. The powder pattern of the form C_{III} ($P2_1/a$), stable at room temperature, is given in Figure 1; the corresponding cell parameters are included in Table I. The existence of three different solid forms clearly follows from Figure 2. The crystal structure determination of C_{III} reveals that the two partner molecules correspond to each other in the same manner

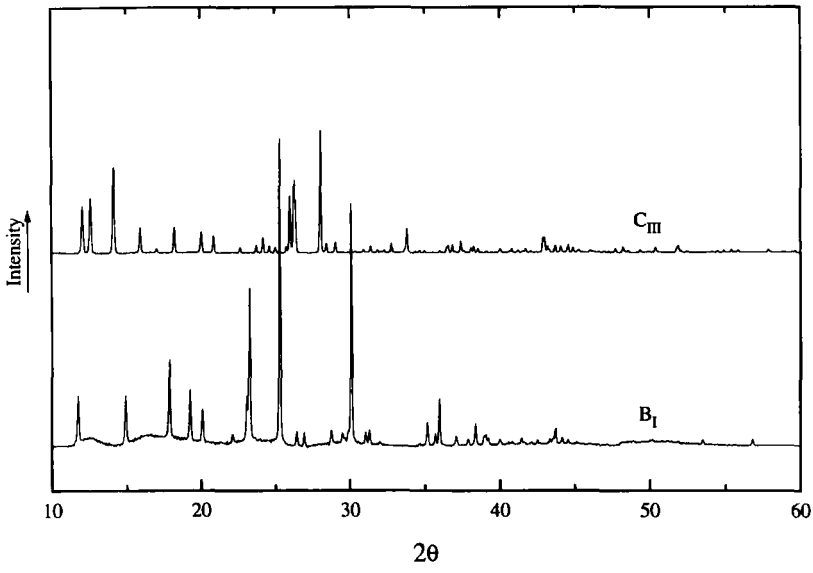

FIGURE 1 Diffraction patterns of the octafluoronaphthalene in its high-temperature form (B_I) and of the complex in its low-temperature form (C_{III}) (λ = 1.54056 Å).

as shown by two layers in the hexagonal graphite structure [43]. The diffraction pattern, Figure 2, does not imply a simple relationship between the structures of C_{III}, C_{II} and C_I. However, from comparable complexes AB, it is known [2] that in the stacking direction (the c-axis) the A, B, A, B sequence is conserved: the 001 reflection of C_{III} is not disappearing at the transitions, so to say. From the rapid attenuation of the C_{II} and C_I reflection lines and considering their small numbers, it follows that C_{II} and C_I are characterized by a considerable thermal motion in combination with high symmetry. It can also be observed that the C_{III} to C_{II} transition is preceeded by an increased thermal expansion, mainly in the a direction as follows from the bending of the 200 line. This phenomenon is also revealed by the thermogram, see Figure 3, in that the ascent from the baseline starts some tens of degrees before the actual transition. A magnification of the evidence is represented by Figure 4, in which the molar heat capacity is plotted against temperature.

The thermodynamic transition data for C are included in Table II. The enthalpy changes involved in the solid-solid transitions are considerable. We may add that the transitions are sharp and take place without delay, no matter the heating rate.

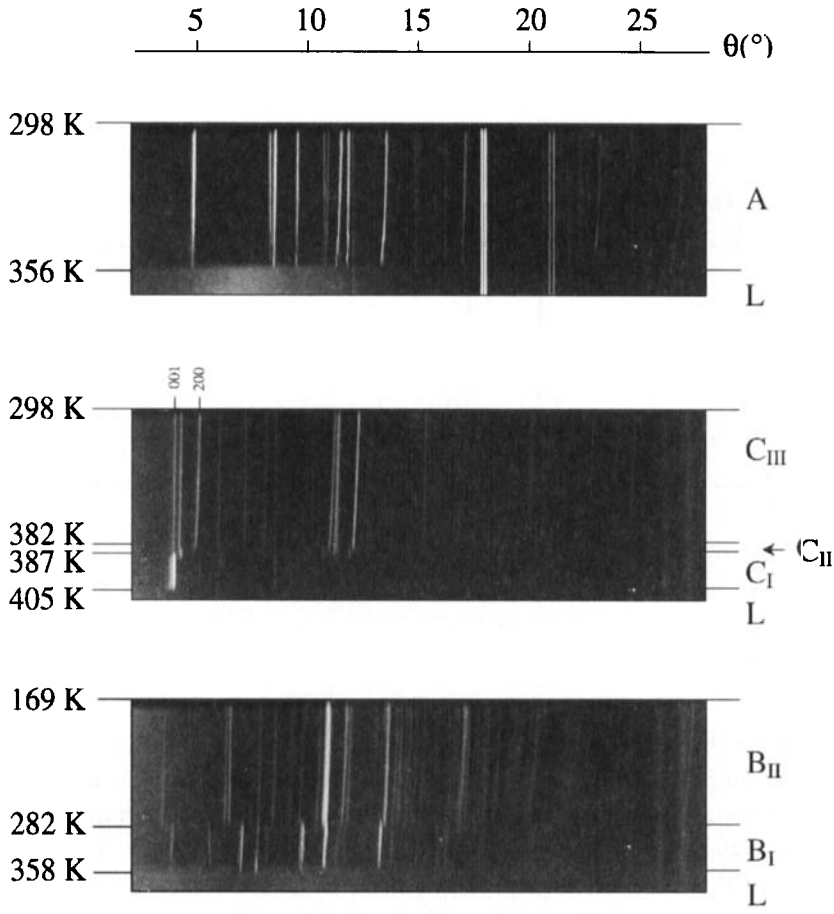

FIGURE 2 Guinier-Simon photographs of naphthalene (*A*), of octafluoronaphthalene (*B*) and of complex (*C*) with increasing temperatures (λ = 1.54056 Å).

III.3. The Experimental Phase Diagram

For several compositions in the system $\{(1-x)$ mole of naphthalene $+ x$ mole of octafluoronaphthalene$\}$, thermal analyses by differential scanning calorimetry and X-ray diffraction as a function of temperature were carried out. The results of these experiments are shown in the *TX* diagram, Figure 5, as far as the relevant temperatures are concerned. In addition, the heat effects measured are shown in Figure 6, along with the so-called Tammann lines. The intersections of these lines with the x-axis yields to the liquid state

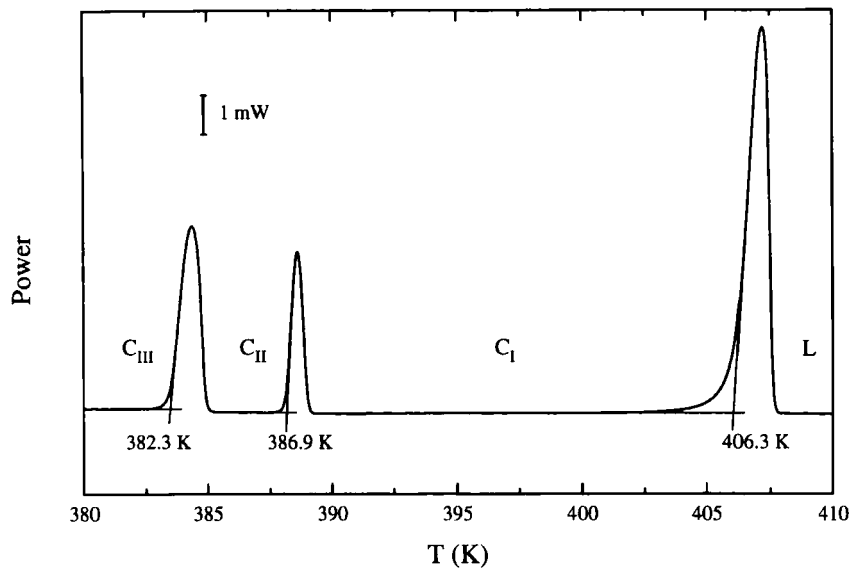

FIGURE 3 Evolution of the differential scanning calorimetry (DSC) curves showing the polymorphism of the complex *C* (4 mg, 2 K·min^{-1}).

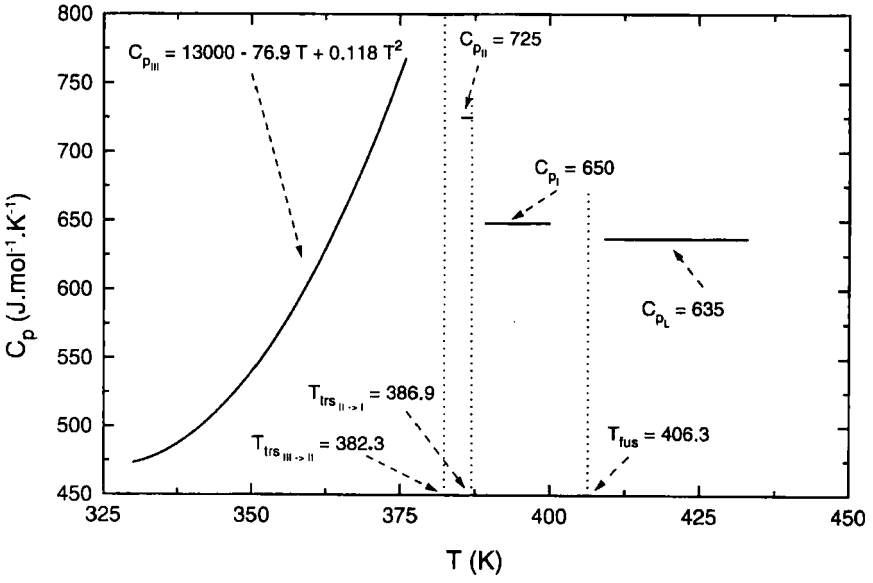

FIGURE 4 Variation with *T* of the calorific capacity of *C* estimated from DSC measurements (4.5 mg, 2 K·min^{-1}).

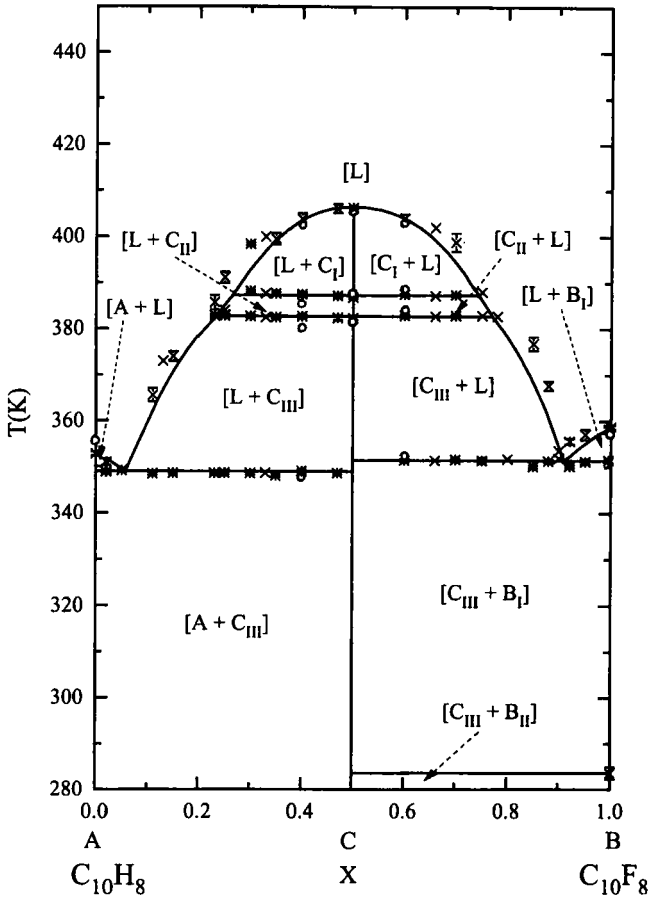

FIGURE 5 Naphthalene-octafluoronaphthalene binary system: comparison between experimental–(o: Guinier-Simon measurements; ⁑ DSC points) and calculated (solid lines) phase diagrams (the optimized parameter values are collected in Tab. III).

boundaries (the metatectic points, M'_1, M'_2, M''_1, M''_2) reported in the first column of the Table III. The intersections of the (E') and (E'') lines give the composition-energy position of respectively E' and E'' eutectics: the corresponding values ($x_{E'}$, $\Delta_{fus}H_{E'}$) and ($x_{E''}$, $\Delta_{fus}H_{E''}$) are reported in Table III. The complete evidence contained in Figures 5 and 6 gives rise to the following remarks:

- the existence of a C complex with a succession of three solid forms is fully confirmed;
- there is neither solid state miscibility, nor non-stoechiometry.

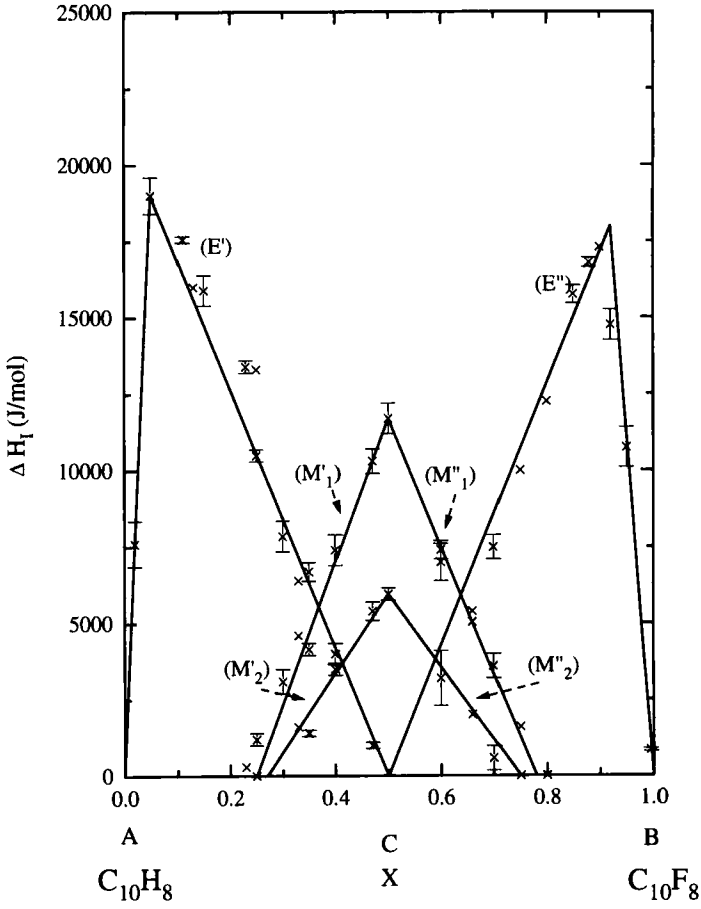

FIGURE 6 Tammann diagrams of the eutectic invariants (E' and E'') and of the invariants related to the C solid-solid transitions (M'_1 and M''_1 at 382.7 K, M'_2 and M''_2 at 387.4 K).

IV. THERMODYNAMIC ANALYSIS

In the case of the system $\{(1-x)$ mole of naphthalene $+\, x$ mole of octafluoronaphthalene$\}$ all solid phases have fixed compositions. As a result, a thermodynamic mixing model is needed for the liquid only. An obvious choice is the associated liquid, which we used before for other complex forming systems and around which one of us [44] constructed the optimization procedure BIMING.

The associated liquid model [45-46] is based on the assumption that the molecular complex only partly dissociates in the liquid state. Consequently,

TABLE III Thermodynamic data of the naphthalene–octafluoronaphthalene system: comparison between experiments and optimization. (units are the $J \cdot mol^{-1}$, the $J \cdot mol^{-1} \cdot K^{-1}$ and the K)

	Experimental values	*Optimized values*
$C_I \rightarrow L$	$\Delta_{fus}H = 26700 \pm 1000$ $T_{fus} = 406.3 \pm 0.3$; $\Delta_{fus}\ C_p = -15(5)$	$\Delta_{fus}H = 27240(100)$ $T_{fus} = 406.5(5)$; $\Delta_{fus}C_p = 0$ $\Delta_f G^0 = -30950(50) + 60(8)T$
$C_{II} \rightarrow C_I$	$\Delta_{trs}H = 5960 \pm 200$ $T_{trs} = 386.9 \pm 0.3$; $\Delta_{trs}\ C_p = -75(20)$ $\Delta_{trs}\ H = 11700 \pm 500$	$\Delta_{trs}H = 5965(10)$ $T_{trs} = 387.4(5)$; $\Delta_{trs}C_p = -50(5)$ $\Delta_{trs}H = 11710(50)$
$C_{III} \rightarrow C_{II}$	$T_{trs} = 382.3 \pm 0.4$ $\Delta_{trs}C_p = -12275(50) + 76.9(10)T$ $-0.118(10)T^2$	$T_{trs} = 382.7(5)$ $\Delta_{trs}C_p = 10(1)$
Liquid		$H^{(1)}_{1,2} = -70(40)\quad S^{(1)}_{1,2} = 0$ $H^{(1)}_{1,2} = 1720(50)\quad S^{(2)}_{1,2} = -10(1)$ $H^{(1)}_{1,3} = 1590(100)\quad S^{(1)}_{1,3} = 0$ $H^{(1)}_{2,3} = 5260(100)\quad S^{(1)}_{2,3} = 0$ $\Delta_{diss}G^0 = 10810(70) - 17(1)(I)$
Metatectic M'_2	$T_{M'_2} = 387.4 \pm 0.5$ $X_{M'_2} = 0.27 \pm 0.02$	$T_{M'_2} = 387.4(5)$ $x_{M'_2} = 0.266(5)$
Metatectic M'_1	$T_{M'_1} = 382.5 \pm 0.4$ $x_{M'_1} = 0.25 \pm 0.02$	$T_{M'_1} = 382.7(5)$ $x_{M'_1} = 0.233(8)$
Eutectic E'	$T_{E'} = 349.0 \pm 0.4$ $x_{E'} = 0.05 \pm 0.02$ $\Delta_{fus}H_{E'} = 19000 \pm 600$	$T_{E'} = 349.0(2)$ $x_{E'} = 0.057(6)$ $\Delta_{fus}H_{E'} = 18770(50)$
Metatectic M''_2	$T_{M''_2} = 387.4 \pm 0.4$ $x_{M''_2} = 0.75 \pm 0.02$	$T_{M''_2} = 387.4(5)$ $x_{M''_2} = 0.743(8)$
Metatectic M''_1	$T_{M''_1} = 382.9 \pm 0.4$ $x_{M''_1} = 0.78 \pm 0.02$	$T_{M''_1} = 382.7(5)$ $x_{M''_1} = 0.770(10)$
Eutectic E''	$T_{E''} = 351.4 \pm 0.4$ $x_{E''} = 0.92 \pm 0.02$ $\Delta_{fus}H_{E''} = 18000 \pm 1000$	$T_{E''} = 351.4(3)$ $x_{E''} = 0.921(5)$ $\Delta_{fus}H_{E''} = 18330(50)$

the mixing enthalpy $\Delta_{mix}H_L$ will be temperature-dependent, as shown experimentally in binary systems such as $C_6H_6 + C_6F_6$, $C_6H_5CH_3 + C_6F_6$ or $1,4\text{-}C_6H_4(CH_3)_2 + C_6F_6$ [10–12]. In this model, interactions between three different species are taken into account: they are A (naphthalene molecules), B (octafluoronaphthalene) and (AB), and they take part in the equilibrium:

$$A + B \rightleftharpoons (AB).$$

In the liquid associated model, the Gibbs energy of mixing is given by:

$$\Delta_{mix}G_L = \sum_{i=1}^{2} \sum_{j=2 j \neq i}^{3} x_i x_j \left[\sum_{\nu=1}^{2} \left(H^{(\nu)}_{i,j} - TS^{(\nu)}_{i,j} \right) (x_i - x_j)^{\nu-1} \right]$$

$$- x_3(\Delta_{\text{diss}}H^0 - T\Delta_{\text{diss}}S^0) + RT\sum_{i=1}^{3} x_i \ln(x_i)/(1 + x_3) \quad \text{(a)}$$

where R is the gas constant and x_i the mole fraction of species i ($i = 1$ for A, $i = 2$ for B and $i = 3$ for (AB)). 12 parameters $H_{i,j}^{(\nu)}$, $S_{i,j}^{(\nu)}$ of the Redlich-Kister type describe the i–j interactions. $(\Delta_{\text{diss}}H^0 - T\Delta_{\text{diss}}S^0)$ is the Gibbs energy of dissociation of the liquid complex (AB). Because monotectic invariants are not present in this binary diagram, we assume that 1–3 and 2–3 interactions do not require second order parameters corresponding to strong repulsive interactions as in inorganic binary systems such as II–VI binaries [45–46]: therefore, $\Delta_{\text{mix}}G_L$ contains 10 parameters.

In the BIMING optimization procedure, the $H_{i,j}^{(\nu)}$ and $S_{i,j}^{(\nu)}$ and parameters of Eq. (a) together with the $\Delta_{\text{diss}}H^0$ and the $\Delta_{\text{diss}}S^0$ constants act as part of the set of adjustable parameters. Phase diagram calculation requires also a description of each solid phase. The Gibbs energy of formation of a phase k from the pure liquid components is assumed to be a function of T:

$$\Delta_f G_k^0 = \alpha_k - \beta_k T + \delta_k T(1 - \ln T), \quad \text{(b)}$$

taking into account a possible change in the heat capacity ΔC_{pk}. For pure components, α_k, β_k and δ_k are given by:

$$\begin{aligned} \alpha_k &= \Delta_{\text{fus}}H_k(T_{\text{fus}_k}) - \Delta C_{pk}T_{\text{fus}_k} \\ \beta_k &= \Delta_{\text{fus}}H_k(T_{\text{fus}_k})/T_{\text{fus}_k} - \Delta C_{pk}\ln T_{\text{fus}_k} \\ \delta_k &= \Delta C_{pk}. \end{aligned} \quad \text{(c)}$$

where $\Delta_{\text{fus}}H_k(T_{\text{fus}_k})$ and ΔC_{pk} are respectively the melting enthalpy and the change in the heat capacity of the component at its melting point T_{fus_k}. These data come from DSC measurements and, then, α_k, β_k, δ_k are not considered as parameters. Possible solid phase transitions may be included by taking into account the enthalpy contribution and the transition temperature.

For the complex, the strategy of finding the parameters, α_C, β_C and δ_C is more complicate. Nevertheless, for fitting the naphthalene + octafluoronaphthalene binary, three constraints were applied [45]. First, for equilibrium between solid and liquid phase, the chemical potential of each component μ_k must be the same in both phases and therefore it was required

that the liquidus temperature at $x = 1/2$ be the melting point of $C(T = T_{\text{fus}_C})$:

$$\mu_A(1/2) + \mu_B(1/2) = \Delta_f G^0_C(T_{\text{fus}_C}).$$

Furthermore, because the left side of this equation is equal to $2\Delta_{\text{mix}} G_L(T_{\text{fus}_C}, 1/2)$, the following relation must be verified:

$$2\Delta_{\text{mix}} G_L(T_{\text{fus}_C}, 1/2) = \Delta_f G^0_C(T_{\text{fus}_C}). \quad \text{(d)}$$

Secondly, the liquid phase is in complete species equilibrium at this liquidus point. This is assured by Eq. (d) and the equation:

$$RT_{\text{fus}_C} \ln a_{L_{(AB)}}(T_{\text{fus}_C}, 1/2) = \Delta_f G^0_C(T_{\text{fus}_C}) \quad \text{(e)}$$

where $a_{L_{(AB)}}(T_{\text{fus}_C}, 1/2)$ is the activity of the (AB) species in these thermodynamic conditions.

The complex melts congruently with a zero change in Gibbs energy. Therefore, the mixing enthalpy of the liquid phase $\Delta_{\text{mix}} H_L$ must satisfy:

$$\Delta_{\text{mix}} H_L(T_{\text{fus}_C}, 1/2) = 1/2[\Delta_{\text{fus}} H + \Delta_f H^0_C(T_{\text{fus}_C})] \quad \text{(f)}$$

($\Delta_f H^0_C(T_{\text{fus}_C})$ represents the enthalpy of formation of the complex from the pure liquid components). The entropy analogue of Eq. (f), that also follows from the zero Gibbs energy of melting, is automatically satisfied when Eq. (d) and Eq. (f) are satisfied.

The two eutectic equilibria:

$$A + C_{\text{III}} \rightleftharpoons L \quad (E')$$
$$B_{\text{I}} + C_{\text{III}} \rightleftharpoons L \quad (E'')$$

give two other constraints. Finally, only 8 independent parameters are required to fit the data. Nevertheless, in the thermodynamic assessment of C_{I}, C_{II} and C_{III} data ($\Delta_{\text{fus}} H$, T_{fus}, $\Delta_{\text{fus}} C_p$, $\Delta_{\text{trs II}\to\text{I}} H$, $T_{\text{trs II}\to\text{I}}$, $\Delta_{\text{trs II}\to\text{I}} C_p$, $\Delta_{\text{trs III}\to\text{II}} H$, $T_{\text{trs III}\to\text{II}}$, $\Delta_{\text{trs III}\to\text{II}} C_p$), the corresponding values are tested during the optimization procedure in order to fit the invariants and the liquidus. According its small value, we take $\Delta_{\text{fus}} C_p$ equal to zero. On the other hand, when optimization starts, the metatectic temperatures are taken to be equal to the respective mean values $T_{M_1} = (T_{M'_1} + T_{M''_1})/2$ and $T_{M_2} = (T_{M'_2} + T_{M''_2})/2$, that which fixes the transition temperatues $T_{\text{trs II}\to\text{I}}$ and $T_{\text{trs III}\to\text{II}}$ respectively. Preliminary fits give $S^{(1)}_{1,2}$ nearly equal to zero. Furthermore, this parameter is taken to be equal to 0. The input data for

the program are all the characteristics of the phase diagram and the thermochemical transition data of the pure components and the complex.

In practice, the "BIMING" routine first optimizes the set of data and verifies the mutual consistency of these data through the minimization of the following F-function:

$$F = 1/(n+2)\sum_{i=1}^{n} w_i\left(\frac{x_{\text{exp}} - x_{\text{cal}}}{x_{\text{exp}}}\right)^2,$$
$$+\sum_{j=1}^{2} w_j\left[\left(\frac{T_{E\text{exp}} - T_{E\text{cal}}}{0.4}\right)^2 + \left(\frac{\Delta_{\text{fus}}H_{E\text{exp}} - \Delta_{\text{fus}}H_{E\text{cal}}}{0.06\Delta_{\text{fus}}H_{E\text{exp}}}\right)^2\right]_j$$

where w_i is the weighting coefficient of the experimental i point on the smoothed liquidus ($n = 80$), w_j the analogue coefficient of the j eutectic point ($T_{E\text{exp}}, x_{E\text{exp}}, \Delta_{\text{fus}}H_{E\text{exp}}$). The phase diagram itself is obtained by minimizing the total Gibbs free energy of the system calculated from Eqs. (a) and (b). The values of parameters given in Table III satisfy the five above constraints and give optimum fit to the liquidus points. The calculated phase diagram is in Figure 5, along with the experimental points.

V. RESULTS AND DISCUSSION

From Table III and Figure 5, it clearly follows that the global agreement between calculated properties and experimental data is quite satisfactory ($F = 0.180$, $<\Delta x> = 0.015$). Very good agreement has been obtained for the metatectic points: the difference between experimental and calculated mole fractions is less than 0.02. Besides, the difference between experimental and calculated melting enthalpies for the eutectic points is less than 350 J/mol.

In terms of the adopted model, the following observations can be made. First of all, there is a strong interaction $A-B$ in the liquid state: for $x = 0.5$ and $T = 406.5$ K the calculated value of the mole fraction of the complex (AB) is 0.28(1). The presence of a strong interaction also finds expression in the calculated enthalpy of mixing, which is $-1.86(3)$ k.J.mol^{-1} for $x = 0.5$ and $T = 406.5$ K. As for the interactions between A and (AB) and between B and (AB), the results imply that the former are less repulsive than the latter ($H_{1,3}^{(1)} < H_{2,3}^{(1)}$, see Tab. III). The difference in the importance of the interactions becomes stronger when the uncombined species compositions (x_1 and x_2) become greater, that means when x or $(1-x)$ increase. This well behaviour in associated liquid (see [45–46]) corresponds to a weak asymmetry with respect to $x = 0.5$ in the calculated phase diagram for the $C_{\text{III}} \leftrightharpoons L$. Because the influence of C_{III} is not x-dependent, this liquidus

asymmetry is related to the liquid properties ($H^{(2)}_{1,2}, H^{(1)}_{1,3}, H^{(1)}_{2,3}$). The part of liquidus curves, involving equilibria with pure components, depends strongly on the slopes at the melting points. As shown by the van't Hoff equations $dT/dx_k(T_{\text{fus}_k})$, these slopes are nearly equal and not very sensitive to a variation of $\simeq 2$ K for T_{fus_k} due to impurities in $C_{10}F_8$. Nevertheless, the starting points of the curves are different: $T_{\text{fus}_A} = 352.8$ K, $T_{\text{fus}_B} = 358.8$ K will then yield to a lower position of the E' eutectic than the one of the E'' eutectic and, then, to a noticeable asymmetry of the phase diagram in the diluted composition ranges.

In the case of the system benzene + hexafluorobenzene, there is also the formation of a 1:1 complex [47]. The available data [10–13] clearly show that the benzene complex is considerably weaker:

- in the benzene system the mole fraction of the complex in the liquid at $T = 297.2$ K is 0.18 and it decreases rather rapidly with temperature; in the naphthalene system it is still 0.28 at $T = 406.5$ K;
- the heat of mixing in the benzene case is $-0.46(1)$ kJ/mol at $x = 0.5$, $T = 297.2$ K, whereas in the naphthalene case it is $-1.86(3)$ kJ/mol at $x = 0.5$, $T = 406.5$ K;
- at its melting point ($T = 297.2$ K) the Gibbs energy of formation of the solid benzene complex from the liquid pure components is $-4.11(1)$ kJ/mol, whereas for the naphthalene complex at its melting point ($T = 406.5$ K) it is $-6.42(2)$ kJ.mol^{-1}; the difference in Gibbs energy of formation finds also expression in the fact the melting temperature of the benzene complex is at a smaller distance from the eutectic three-phase equilibria ($\simeq$30 K) than in the case of the naphthalene complex ($\simeq$50 K).

The highly polymorphic nature of the complex naphthalene + octafluoronaphthalene can be explained, as in the benzene + hexafluorobenzene system [47], by the easiness with which molecules turn in their planes. We can expect an analogue behaviour with decreasing temperatures: in a structural point of view, the sequence I → II → III would correspond, for the C_I phase, to molecules turning around their sticking axis; in the C_{II} phase, the rotation of $C_{10}F_8$ molecules would be frozen out; finally, in the C_{III} phase, any molecule rotations would be frozen out.

VI. CONCLUSION

By conclusion, we have shown that the 1:1 complex in the system naphthalene + octafluoronaphthalene is more stable than its analogue in

the system benzene + hexafluorobenzene. All pertinent thermodynamic data have been evaluated and assessed, showing a greater association character of the liquid phase. This complex stability both in solid- and liquid phases may be related to the eight possible $H \ldots F$ interactions between naphthalene and octafluoronaphthalene. Because of the lack of results on the polymorphism of the solid complex, structural studies are needed for understanding the two solid–solid transition mechanisms and the corresponding enthalpy changes.

References

[1] C. R. Patrick and G. S. Prosser, *Nature*, **187**, 1021 (1960).
[2] J. C. A. Boeyens and F. N. Herbstein, *J. Phys. Chem.*, **69**(7), 2153 (1965).
[3] W. A. Duncan and F. L. Swinton, *Trans. Faraday Soc.*, **62**, 1082 (1966).
[4] D. F. R. Gilson and C. A. McDowell, *Can. J. Chem.*, **44**, 945 (1966).
[5] E. McLaughlin and C. E. Messer, *J. Chem. Soc.*, **A**, 1106 (1966).
[6] W. A. Duncan and F. L. Swinton, *J. Phys. Chem.*, **70**(7), 2417 (1966).
[7] S. Miyagishi, A. Isomi, M. Iwata, T. Asakawa and M. Nishida, *Bull. Chem. Soc. Jpn.*, **58**, 3643 (1985).
[8] W. A. Duncan, J. P. Sheridan and F. L. Swinton, *Trans. Faraday Soc.*, **62**, 1090 (1966).
[9] R. J. Powel and F. L. Swinton, *J. Chem. Therm.*, **2**, 87 (1970).
[10] D. V. Fenby, I. A. McLure and R. L. Scott, *J. Phys. Chem.*, **70**(2), 602 (1966).
[11] D. V. Fenby and R. L. Scott, *J. Phys. Chem.*, **71**(12), 4103 (1967).
[12] A. Andrews, K. W. Morcom, W. A. Duncan, F. L. Swinton and J. M. Pollock, *J. Chem. Thermodynamics*, **2**, 95 (1970).
[13] A. Marbeuf, D. Mondieig, V. Metivaud, Ph. Negrier, M. A. Cuevas-Diarte and Y. Haget, *Mol. Cryst. Liq. Cryst.*, **293**, 309 (1997).
[14] W. J. Gaw and F. L. Swinton, *Nature*, **212**, 283 (1966).
[15] W. J. Gaw and F. L. Swinton, *Trans. Faraday Soc.*, **64**, 637 (1968).
[16] W. J. Gaw and F. L. Swinton, *Trans. Faraday Soc.*, **64**, 2023 (1968).
[17] E. M. Dantzler and C. M. Knobler, *J. Phys. Chem.*, **73**(5), 1602 (1969).
[18] E. Bartsch, H. Bertagnolli and P. Chieux, *Ber. Bunsenges Phys. Chem.*, **90**, 34 (1986).
[19] T. G. Beaumont and K. M. S. Davis, *J. Chem. Soc.*, (**B**); *Phys. Org.*, 1131 (1967).
[20] P. R. Hammond, *J. Chem. Soc.*, (**A**), 145 (1968).
[21] M. E. Baur, D. A. Horsma, C. M. Knobler and P. Perez, *J. Phys. Chem.*, **73**(3), 641 (1969).
[22] M. E. Baur, C. M. Knobler, D. A. Horsma and P. Perez, *J. Phys. Chem.*, **74**, 4594 (1970).
[23] N. M. D. Brown and F. L. Swinton, *J. Chem. Soc., Chem. Commun.*, 770 (1974).
[24] J. Hernandez-Trujillo, M. Costas and A. Vela, *J. Chem. Soc. Faraday Trans.*, **89**(14), 2441 (1993).
[25] S. W. Overell and G. S. Pawley, *Acta Cryst.*, **B38**, 1966 (1982).
[26] T. Dahl, *Acta Chem. Scand.*, **25**(3), 1031 (1971).
[27] T. Dahl, *Acta Chem. Scand.*, **26**(4), 1569 (1972).
[28] T. Dahl, *Acta Chem. Scand.*, **27**(3), 995 (1973).
[29] Y. Haget, L. Bonpunt, F. Michaud, Ph. Negrier, M. A. Cuevas-Diarte and H. A. J. Oonk, *J. Appl. Cryst.*, **23**, 492 (1990).
[30] D. Mikailitchenko, A. Marbeuf, Y. Haget and H. A. J. Oonk, *Mol. Cryst. Liq. Cryst.*, to be published.
[31] D. Mondieig, A. Marbeuf, C. Dalari, P. Negrier, J. M. Leger and Y. Haget, *XXI Jeep* (Rouen, 1995), p. 276.
[32] F. P. Chen and P. N. Prasad, *Chem. Phys. Lett.*, **47**(2), 341 (1977).
[33] F. P. Chen and P. N. Prasad, *Chem. Phys. Lett.*, **34**(2), 219 (1978).

[34] R. Couchinoux, N. B. Chanh, Y. Haget, M. T. Calvet, E. Estop and M. A. Cuevas-Diarte, *J. Chim. Phys.*, **86**, 561 (1989).
[35] Y. Haget, H. A. J. Oonk and M. A. Cuevas-Diarte, *XVI Jeep* (Marseille, 1990), p. 35.
[36] A. Del Pra, *Acta Cryst.*, **B28**, 3438 (1972).
[37] N. A. Ahmed, *Zh. Stroukt. Khim.*, 573 (1973).
[38] G. S. Pawley and O. W. Dietrich, *J. Phys. C: Solid State Phys.*, **8**, 2549 (1975).
[39] G. A. McKenzie, J. W. Arthur and G. S. Pawley, *J. Phys. C: Solid State Phys.*, **10**, 1133 (1977).
[40] F. P. Chen and P. N. Prasad, *Chem. Phys. Lett.*, **45**(2), 373 (1977).
[41] G. A. McKenzie, B. Buras and G. S. Pawley, *Acta Cryst.*, **B34**, 1918 (1978).
[42] D. M. Adams, A. C. Shaw, G. A. McKenzie and G. S. Pawley, *J. Phys. Chem. Solids.*, **41**, 149 (1980).
[43] J. Potenza and D. Mastropaolo, *Acta Cryst.*, **B31**, 2527 (1975).
[44] A. Marbeuf, *Logiciel* "Biming" (Agence Nationale du Logiciel, Paris, 1991).
[45] T. Tung, C.-H. Su, P.-K. Liao and R. F. Brebrick, *J. Vac. Sci. Technol.*, **21**, 117 (1982).
[46] A. Marbeuf, R. Druihle, R. Triboulet and G. Patriarche, *J. Cryst. Growth*, **117**, 10 (1992).
[47] J. H. Williams, J. K. Cockcroft and A. N. Fitch, *Angew. Chem. Int. Ed. Engl.*, **31**, 1655 (1992).